Graphene-based Filtration Media for Spacecraft Potable Water Systems: An Early Investigation

Rogelio E. Garcia Fernandez*
Jacobs Technology Inc., Houston, Texas, 77058

Michael Callahan†
NASA Johnson Space Center, Houston, TX, 77058, USA

and

Luke Gurtowski‡
U.S. Army Engineer Research and Development Center, Vicksburg, Mississippi, 39180

Graphene-based materials have allowed fundamental advances in fields such as energy storage, electronics development, material science, optics, medicine, and water processing due to their unique two-dimensional structure, mechanical robustness, large surface, and high conductivity. However, little to no effort has been devoted to exploiting and studying these materials to develop new water technologies suited for spacecraft applications. One such application is the potential use of graphene-based materials as filtration media for reclaimed water. Therefore, studying the adsorptive performance of these new materials becomes crucial in identifying the opportunity to replace/upgrade state-of-the-art filtration media currently used in space vehicles with water recovery capability; especially if consumable requirements can be lessened as a result of extended filtration capacity. This early Life-Support-Systems investigation pioneers in graphene research by testing a number of graphene-based materials in comparative adsorption and antimicrobial experiments where contaminant removal efficiency, maximum adsorption capacity, and bacterial reduction are probed. This preliminary investigation informs on the practicality of using graphene-based materials as filtration media and provides a discussion on the scaling-up and optimization of this prospective filtration technology for spacecraft potable water systems.

Nomenclature

ACTEX	= Activated Carbon Ion Exchange	*MF*	= Multifiltration
$C_3H_8O_2$	= propylene glycol	$(NH_4)HCO_3$	= ammonia bicarbonate
C_{ct}	= contact time	NH_4^+	= ammonium ion
C_e	= equilibrium concentration	q	= specific adsorption capacity
C_i	= initial adsorbate concentration	q_e	= equilibrium adsorption capacity
GACT	= Graphene-based Adsorption Capacity Tests	q_{max}	= maximum adsorption capacity
GBM	= Graphene-Based Materials	R^2	= coefficient of determination
GNP	= Graphene Nanoplatelets	*SOTA*	= State-Of-The-Art
IC	= Ion Chromatography	t	= time
ICES	= International Conference on Environmental Systems	*TIC*	= Total Inorganic Carbon
		TOC	= Total Organic Carbon
ISS	= International Space Station	*V*	= volume of solution
K	= kinetic constant	*WPA*	= Water Processor Assembly
LSS	= Life Support Systems	η	= removal efficiency

* Life Support Systems Test Engineer, JETS II Contract, Jacobs Engineering, 2224 Bay Area Blvd, Mail Stop: JE4EA.
† Water Technology Lead, Crew and Thermal Systems Division, 2101 E NASA Pkwy, Mail Stop: EC3.
‡ Research Chemical Engineer, Environmental Engineering Branch, 3909 Halls Ferry Rd, Mail Stop: Bldg. 3297.

I. Introduction

Graphene is a one-carbon-atom-tick material first synthesized from graphite by Gem et al. in 2004 using the "scotch tape" method.[1] The isolation of this two-dimensional material allowed the material science community to experimentally confirm the theoretically-predicted high electron mobility (200,000 cm^2/Vs)[2], optical transparency (97.4%)[3], thermal conductivity (3000-5000 Wm/K)[4], mechanical strength (1.0 TPa)[5], and specific surface area (~2600 m^2/g)[6] exhibited by graphene. The synthesis of stable mono-layer graphene permitted its reconfiguration into different Graphene-based Materials (GBM), such as graphene oxide, reduced graphene, functionalized graphene, graphene composites, graphene aerogels/hydrogels, and superficially graphene-loaded materials. These materials have been extensively researched for a wide range of applications, with water treatment being no exception. For instance, various investigations have fundamentally studied the sorption performance of GBM for toxins[7], pharmaceuticals[8], water-soluble organics[9], volatile compounds[10], heavy metals[11], nuclear-waste constituents[12], oils[13], and dyes[14], reporting noteworthy contaminant removal levels. Moreover, GBM have been identified as potential materials for antimicrobial applications in water environments. Nevertheless, microbial reduction by graphene has only been studied for a limited number of bacterial species, and clear physiochemical mechanisms have not been entirely developed to explain this reported antimicrobial property.[15–17]

Despite the advancements made in developing new materials and technologies using GBM for water treatment in terrestrial applications, the physiochemical properties of these materials have been minimally studied in terms of their potential ability to remove specific contaminants found in spacecraft life support systems (LSS). A keyword search for “graphene” in the paper repository provided the International Conference in Environmental Systems (ICES) indicates that graphene-based technologies have only being considered for thermo-mechanical applications.[18] The promising adsorption performance of GBM across a wide range of water contaminants and its potential antimicrobial capacity has sparked interest in researching these materials for water filtration capabilities in spacecraft LSS, especially since tailored graphene-based filtration media could overcome limitations imposed by state-of-the-art (SOA) spacecraft water technologies and ecologically-specific contaminants.

Currently, the Water Processor Assembly (WPA) aboard the International Space Station (ISS) can be regarded as the SOA process unit for spacecraft Water Recovery Systems (WRS). The WPA processes wastewater through a series of processing steps, such as phase separation, physical/chemical filtration, heating/cooling, oxidation, ion exchange, and disinfection. Matured graphene-based water technologies could improve such systems by serving as filtration media with higher removal capacity for organic and inorganic impurities, as well as possible treatment and/or removal of microbial loads. In the WPA, the majority of the water-soluble contaminants are removed by ion exchange and adsorption media contained in the Multifiltration (MF) beds. However, supply of the MF beds can represent a significant mass requirement (~up to 14.0 kg).[19] On the other hand, microbes present in the process water that manage to pass through the MF beds are primarily eliminated through a subsequent step of high-temperature oxidation. Following this step, a residual biocide is introduced to inhibit any microbial growth in the product water.[20] Future WPA-like units may be optimized for extended reliability and used for longer manned missions to the moon or Mars if graphene-based filtration media contains a single versatile adsorbent with enhanced removal capabilities for microbes, ionic and nonionic organics, and inorganics. Consequently, in order to determine if there is a potential for improving water-filtration technologies through the utilization of graphene, a trade study was conducted to compare the adsorptive and antimicrobial properties of graphene and GBM with SOA filtration media.

Pristine graphene is theoretically regarded as an exceptional adsorbent for a variety of adsorbates due to its large natural surface area. Some studies have been able to produce graphene grades with high surface areas ranging between 2640-3355 m^2/g.[21,22] Since this material has an authentic two-dimensional structure and/or is comprised of highly-accessible nanostructures, most of its surface would be active/available for adsorption provided good contact with the adsorbate-carrying phase. In contrast, SOA particles consist of spherical beads with macropores, mesopores, and micropores whose interior active surface is susceptible to diffusion-based transport limitations. This obstruction might limit the active surface area of SOA filtration media. The WPA MF beds incorporate two engineered particles: AmberSorb® 4652 for organic removal and AmberLite® IRN-150, IRN-77, IRA67 for removal of ionic contaminants as described by Kayatin et. al.[19] Despite the potential increase in active surface area resulting from its geometric conformation, graphene only comes in the form of nano powder/platelets, which are aggregates of graphene layers with a thickness of a few nanometers and a width of a couple of micrometers. Hence, available pristine graphene particles cannot be instantaneously consolidated into a flow-thought packed bed for testing since the minuscule powder will require high pressure drop for normal system flow rates. Nevertheless, the adsorption capacity of graphene for spacecraft water contaminants has not yet been extensively studied by a research group that focused on spacecraft life

support systems, and this effort constitutes an opportunity to study potential "next-generation" filtration media for SWRS applications.

This early investigation intends to pioneer in graphene research for spacecraft WRS applications by conducting a series of adsorption capacity tests with different grades of commercially-available GBM products. The Graphene-based Adsorption Capacity Tests (GACT) seeks to provide the necessary metrics to estimate the maximum (apparent) adsorption capacity of GBM for a selection of WRS-related contaminants. The adsorption capacity is the amount of adsorbate taken up by the adsorbent per unit mass (or volume) of the adsorbent. This parameter will be compared to the corresponding values for SOA media. Furthermore, this effort performed a sequence of preliminary antimicrobial tests to investigate the effectiveness of GBM in suppressing microbial growth in water. The knowledge acquired throughout this investigation offer a foundation for the practical application of GBM as a filtration material in the context of water recovery operations in spaceflight, as well as initial parameters for optimizing and scaling up graphene-based water filtration technology.

II. Materials and Methods

The GACT consisted of batch-mode experiments in which contaminated water is allowed to interact with a predetermined load of filtration media in mixing conditions over a specific contact time. By measuring the contaminant (adsorbate) concentration at different contact times and adsorbent loads, isotherm diagrams were constructed to visualize the adsorption process at equilibrium. Similarly, the same measurements were used to build an adsorption-kinetics diagram describing the transient characteristic of the apparent adsorption process. For both data-representation schemes, the specific adsorption capacity can be computed for a range of contact times and adsorbent loads at a fixed adsorbate loading; this metric is calculated as

$$q = \frac{(C_i - C_{ct})V}{m} \tag{1}$$

where C_i, C_{ct}, V, and m are the initial adsorbate concentration (mg/L), the adsorbate concentration (mg/L) at a specific contact-time, the volume of the solution (L), and the mass of the adsorbent (mg), respectively. Eq. 1 also computes the equilibrium adsorption capacity (q_e) when "C_{ct}" reaches a saturation point or equilibrium concentration (C_e). When q_e is plotted against C_e, the graph reveals an isotherm. In addition, adsorption kinetics for each experimental condition can be visualized by plotting q vs. time (t, [min]). By building the linearized forms of these plots, mathematical models can be employed to fit the data following a degree of regression and to calculate the corresponding maximum adsorption capacity (q_{max}) or the kinetic constant (K). The GACT utilized the adsorption models (and their linearized expressions) listed in Table 1 to determine limiting adsorption pathways and the respective mathematical coefficients. In addition, the experimental data was used to determine the contaminant/adsorbate removal efficiency (η), computed using Eq. 2 and used to describe how much contaminant (%) was removed at a discrete adsorbate concentration point. It is worth highlighting that the different K-constants provided in Tablet 1 correspond to a specific model (see subscripts) and comprise of different dimensionalities.

$$\eta = \frac{C_i - C_{ct}}{C_i} \times 100\% \tag{2}$$

Table 1. Adsorption Models and Their Linearized Expressions

Adsorption Model	Expression	Linear Expression	Plot
Langmuir[23]	$q_e = q_m\left[\frac{K_L C_e}{1 + K_L C_e}\right]$	$\frac{1}{q_e} = \left[\frac{1}{K_L q_m}\right]\left[\frac{1}{C_e}\right] + \frac{1}{q_m}$	$\frac{1}{q_e}\ vs.\ \frac{1}{C_e}$
Freundlich[24]	$q_e = K_F C_e^{1/n}$	$ln(q_e) = ln(K_f) + \frac{1}{n} ln(C_e)$	$ln(q_e)\ vs. ln(C_e)$
pseudo-1st order kinetic[25,26]	$q = q_e^{\left(1-e^{-K_1 t}\right)}$	$\ln(q_e - q) = -K_1 t + ln(q_e)$	$\ln(q_e - q)\ vs. t$
pseudo-2nd order kinetic[27]	$q = \frac{K_2 t q_e}{K_2 t + 1}$	$\frac{t}{q} = \left[\frac{1}{q_e}\right] t + \frac{1}{K_2 q_e^2}$	$\frac{t}{q}\ vs. t$
intraparticle diffusion[28,29]	$q = K_{id} t^{0.5}$	$q = K_{id} t^{0.5} + s$	$q\ vs. t^{0.5}$

s: thickness of the boundary layer

A. GACT Materials

The GACT collected experimental data based on a matrix of adsorbates and adsorbents. The adsorbates included inorganics and/or organics found in ISS wastewater streams. To narrow down graphene's affinity to certain contaminants and to meticulously understand how the nature of the contaminant affects the adsorption process, single-component aqueous solutions were prepared to initiate the benchtop adsorption experiments. The main inorganic and organic contaminants were ammonia bicarbonate ($(NH_4)HCO_3$) and propylene glycol ($C_3H_8O_2$), respectively. These molecules were selected as absorbates because they have the highest contaminant concentration in ISS reclaimed water as described by Muirhead et al.[30] Additionally, their solutions can be prepared easily and stored stably. Another organic molecule, 2-(2-Butoxyethoxy)Ethanol (162.23 g/mol), was selected as a backup option since it was hypothesized that $C_3H_8O_2$ might not be readily taken up by the adsorbents in these scaled-down experiments due to its inherent low molecular weight. This organic molecule is also present in the recipe described by Muirhead et al. and has the highest molecular weight. Throughout the GACT, the $(NH_4)HCO_3$ concentration was quantified based on the concentration of its respective cation via Ion Chromatography (IC) measurements. The concentration of organic molecules was measured as Total Organic Carbon (TOC) via high temperature catalytic oxidation. The available instrumentation for this analytical technique also provided Total Inorganic Carbon (TIC) metrics, which were also used during the adsorption-based modeling. The initial concentration of the NH_4^+, TIC, and TOC in the contaminant solutions were 100 mg/L, 90 mg/L and 6 mg/L respectively. Moreover, the GACT selection of adsorbents (Figure 1) was based on existing SOA media inventory and in-stock grades of graphene. The purpose of this selection was to compare the performance of GBM against SOA products. The GACT incorporated the following adsorbates: xGnP® 750 m^2/g Graphene Nanoplatelets (GNP), Graphene Supermarket® granulated graphene, UltraClean™ UCW 3600 (by Purolite™), and AmberSorb™ 4652 (by Dow Chemical Company). Note that AmberLite® IRN-150, IRN-77, IRA67 were not tested in this study since these products were not available. UltraClean™ UCW 3600 (formerly known as Purolite® NRW36) was chosen as the SOA ion-exchange-based filtration media for this research, as it is utilized in the Activated Carbon Ion Exchange (ACTEX) cartridge for water filtration in the ISS oxygen generation assembly.[31]

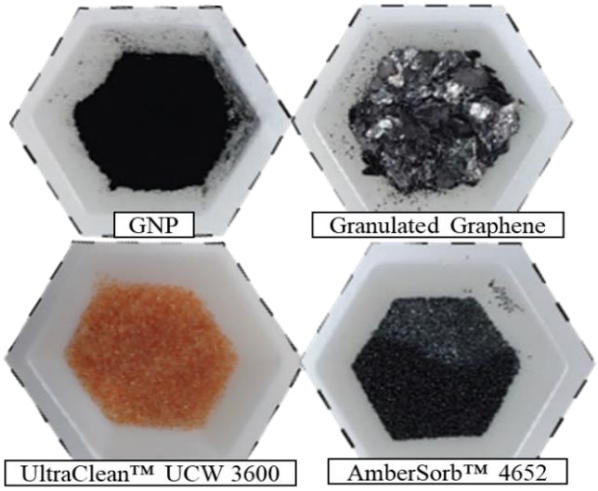

Figure 1. GACT Adsorbents.

B. GACT Methodology

The adsorption experiments were carried in batch mode with moderate mixing mediated by magnetic stirring (Figure 2). Using sealed glass jars, the selected adsorbates and adsorbents were allowed to interact for a predetermined contact time. The GACT testing matrix consisted of an array of increasing contact times, an array of varying adsorbent loads, and a fixed contaminant concentration. The adsorbent (adsorption media) amount in the experiments ranged from 50-6400 mg. Each jar was assigned a contact time (5 min, 15 min, 30 min, 60 min) and accommodated enough volume for the extraction of quadruplicated samples. Therefore, 0.2 L of adsorbate mix (contaminant solution) was added to each contact-time-assigned jar since this volume allowed the chosen sample replication and the minimum volume required by the IC (10 mL) and TOC (40 mL) analyzers. When a contact time was reached, aliquots were withdrawn from the jar using a sterile syringe and transferred to a test tube after a filtration step using a 0.2 µm nylon filter. Since GNP generated well-dispersed suspensions that rapidly saturated syringe filters, the aliquots were placed

in a centrifuge at 5000 revolutions per minute for five minutes. Finally, the subsequent supernatant obtained from the centrifugation process was gathered and subsequently filtered in order to prepare the ultimate water volume for analytical examination.

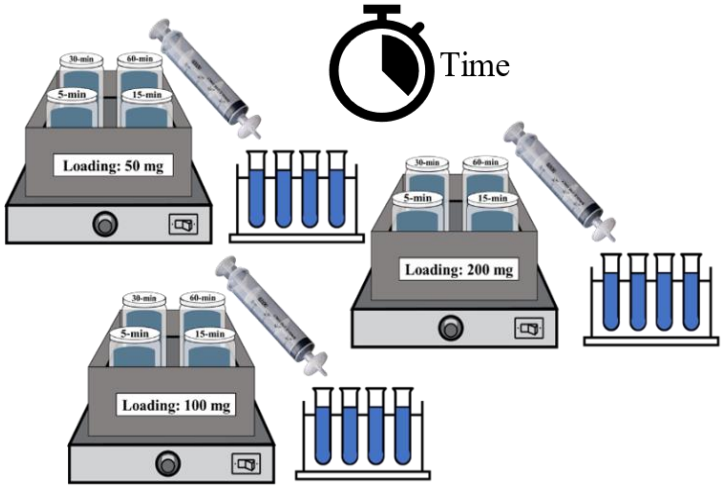

Figure 2: Experimental Setup for the Graphene Adsorption Capacity Test.

C. Microbial Challenge Test

GNP and AmberSorb™ 4652 were added to 20 mL of sterilized deionized water in a 50 mL polypropylene conical tube at varying concentrations: 0 mg/200mL (control), 100 mg/200 mL, 400 mg/200 mL, 1600 mg/200 mL, and 6400 mg/200 mL. Burkholderia Multivorans (accession number 172630038-1, isolated from ISS WPAwastewater) was added to each tube at a final concentration of approximately 106 CFU/mL, and the tubes were vortexed for 10 seconds to ensure complete mixing. Samples (100 µL) from each tube were removed for enumeration of the starting bacterial concentration of each solution, and the remaining solution was incubated at 35°C in a shaking incubator at 150 RPM and a 15° incline. Samples (100 µL) were removed from each tube after 1 hr., 2 hr., and 3 hr. of incubation to enumerate the bacterial concentration over time. These samples were serially diluted in Butterfield's buffer and spread plated on R2A agar. Plates were incubated at 35°C for 2 days and counted. Each experiment was repeated 3 times, and the control solution was normalized to a 106 CFU/mL concentration at all time points.

III. Results and Discussion*

First, absorption capacity (q) and removal efficiency (η) values were calculated by analyzing the anticipated and inherent performance of the adsorbents in removing specific pollutants. For example, AmberSorb™ 4652 was not intentionally tested with $(NH_4)HCO_3$ solutions since the adsorption properties of its activated-carbon nature are not based in ion-exchange mechanisms, which are more suitable than sorption processes for the removal of inorganic substances like ammonium ion (NH_4^+) or Total Inorganic Carbon (TIC). Similarly, q and η metrics are not discussed in this section in relation to the adsorption of organic compounds by UltraClean™ UCW 3600 because this product is predominantly marketed for the removal of ionic contaminants. Therefore, the experimental design did not incorporate tests involving this particular adsorbent and organic contaminants. Moreover, the first experiments with $C_3H_8O_2$ solutions did not provide a broad set of data sufficient for analysis. Therefore, these results are not presented here. Although the initial $C_3H_8O_2$ concentration could have been optimized to a very-high value that compensated this molecule's low molecular weight and allowed measurable changes in concentrations due to the adsorption process, this effort was not pursue since the required tunability might have resulted in a time-consuming endeavor. Instead,

* The testing conducted in the scope of this study was carried out in accordance with internally developed procedures and methodologies, solely aimed at gathering data for the preliminary evaluation of the adsorption capacities and/or kinetics of the tested materials under similar conditions. Consequently, the results presented in this paper should not be utilized for the purpose of directly comparing the performance of SOA filtration media with existing system-level test data or vendor information.

organic contaminant solutions were changed by using 2-(2-Butoxyethoxy)Ethanol. Figures 3, 4, 5 and 6 summarize the results for the adsorption of NH_4^+, TIC, and TOC (at different adsorbent loads).

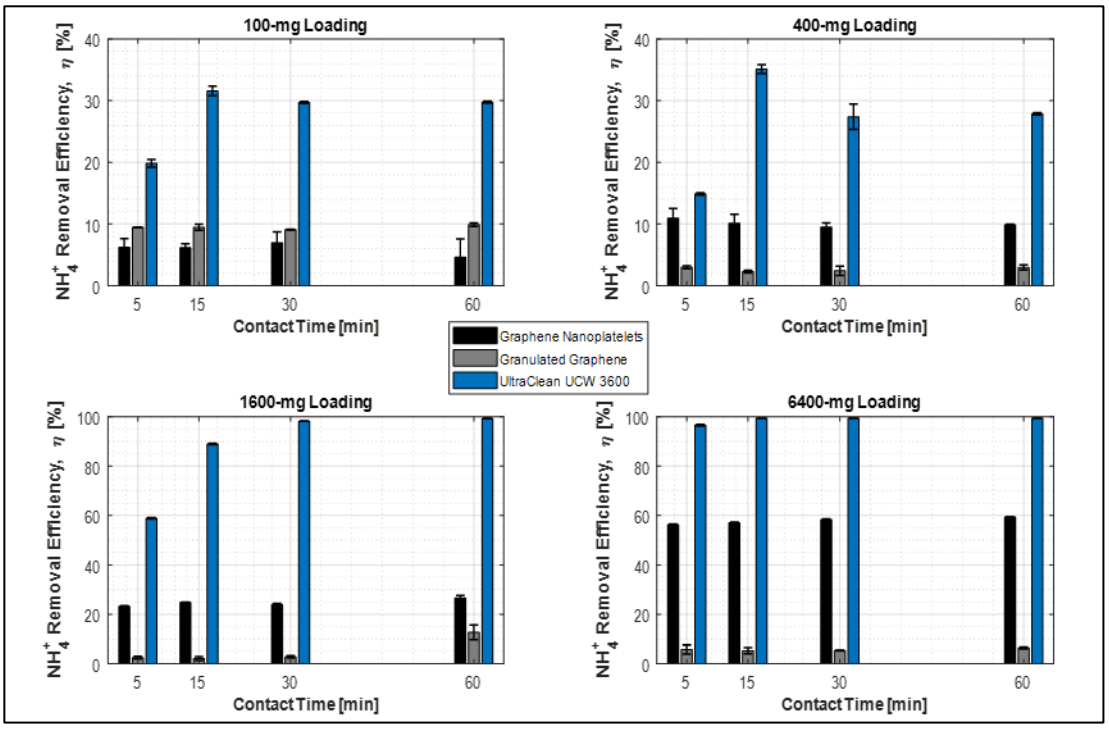

Figure 3. NH4+ Removal Efficiency versus Contact Time at Different Adsorbate Loadings.

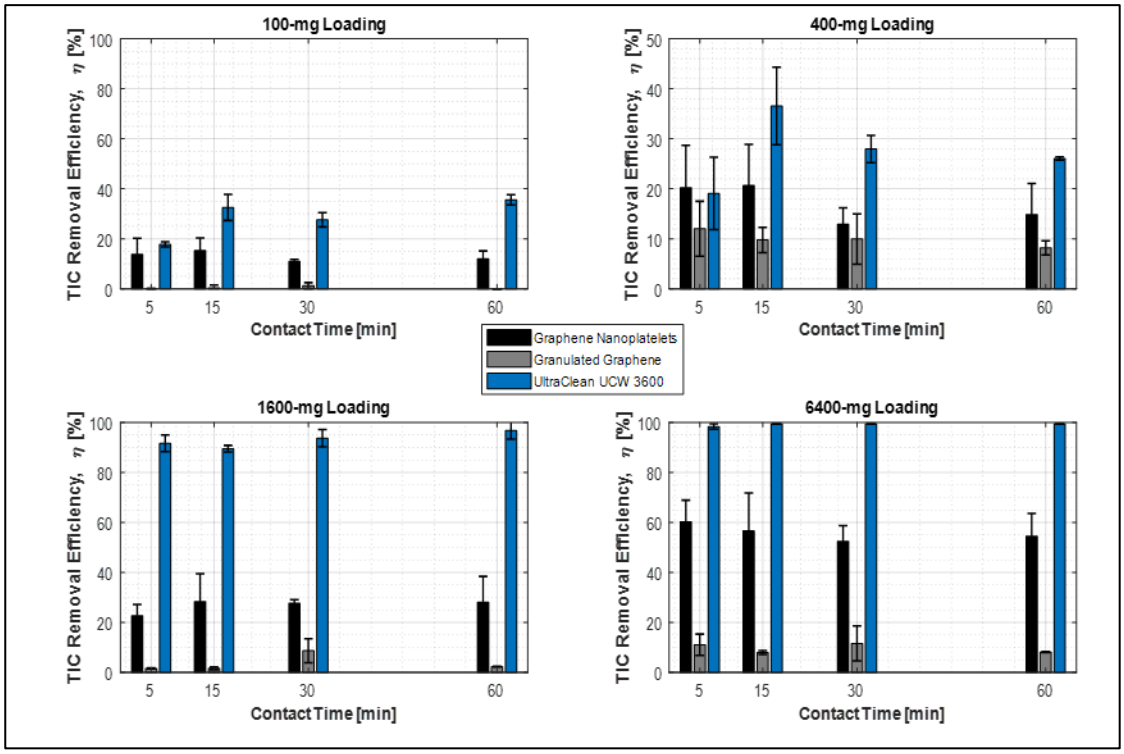

Figure 4. TIC Removal Efficiency versus Contact Time at Different Adsorbate Loadings.

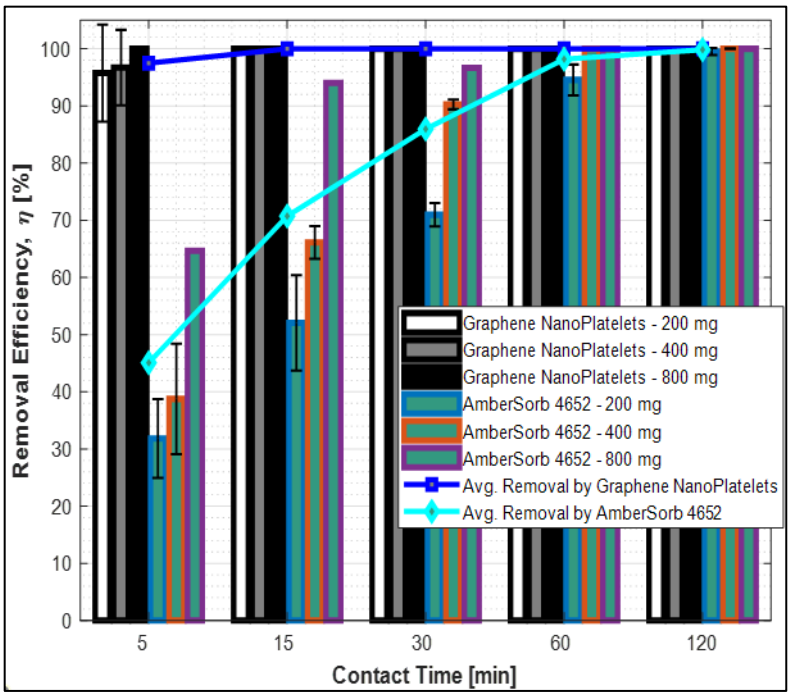

Figure 5. TOC [6.0 mg/L] Removal Efficiency vs. Contact Time at Different Loadings.

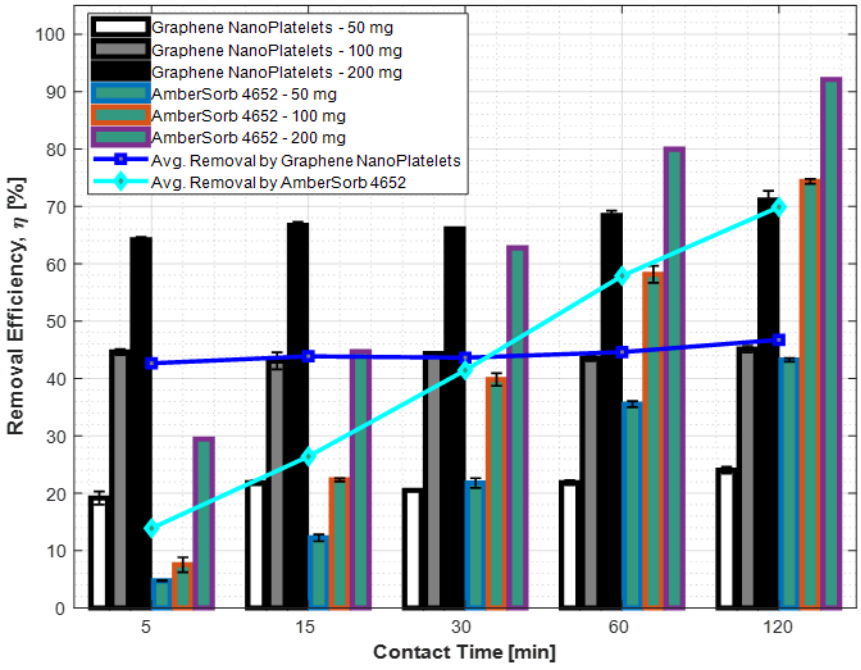

Figure 6. TOC [40.0 mg/L] Removal Efficiency vs. Contact Time at Different Loadings

As expected, Figure 3 shows that the removal of $NH4^+$ is enhanced as the adsorbate loading increases. Surprisingly, the 100-mg result in the same figure reveals that granulated graphene removed more $NH4^+$ than GNP by a few percents; however, the granulated form of the adsorbate did not respond with higher removal percentages relative to the GNP as loading increased. Granulated Graphene is made by rolling GNP to create larger pieces of graphene material; the surface area of the precursor GNP is unknown. Knowing the specific volume-to-material ratio at which

the expensive GNP and the more affordable granulated graphene exhibit similar performance is beneficial for experimental purposes. The results in Figure 3 might indicate that these two materials reached the same performance at a volume-to-material ratio close or below 100 mg/200 mL. More significantly, Figure 3 demonstrates that the GBM did not surpass the absorption efficiency of UltraClean™ UCW 3600 at any test point. It merits attention that this result is not concerning since the pristine GNP did not have any chemical functionalization that allowed a competitive performance against the SOA ion-exchange resin. This SOA adsorbate behaved nicely at removing more NH_4^+ as the loading increased. Note that the metrics for GNP in Figure 3 maintained a close η level at each contact time, and the charts did not capture an obvious transient phase. This trend, which is also seen in Figure 4, might indicate that the GNP had reached its specific adsorption capacity for these loadings. Therefore, the selected the data resolution for the contact-times selected might not have been sufficient to fully capture a well-defined time-dependent correlation.

In a similar fashion, Figure 5 shows how quickly GNP removed all of the organic contaminant at each TOC contaminant loading. Figure 5 compiles the η for GNP and AmberSorb™ 4652 at three different material loadings as well as the averaged performance (n=3) from three-loading experiments. Note that Granulated Graphene loadings did not remove any TOC during the experiments, so the corresponding results are not plotted. The results for GNP are constrained for the q_{max} estimation since the metrics were not diverse enough for a linearized isotherm or kinetic-based analysis. In contrast, the same figure illustrates the desired removal trend with the performance of the SOA adsorbent. Although AmberSorb™ 4652 provided dispersed metrics, these results were not further processed for theoretical parameter estimation since the corresponding GNP data was unsuitable for analysis. However, the ability of GNP to remove the same amount of TOC faster than the SOA material was considered a compelling and attractive result that might be considered for specific types of applications. Furthermore, the concentration of the TOC, as 2-(2-Butoxyethoxy)Ethanol, was increased to 40.0 mg/L to resolve the 100%-η performance of GNP observed in Figure 5. (Recollect that only diverse η values across different loading and contact-time conditions allow for the deployment of the linearized adsorption models). Hence, the GACT experiments were repeated with this new initial TOC level.

Figure 6 presents a set of results that are more suitable for isotherm and/or kinetics analysis since η values have a better distribution over the selected experimental conditions. Specifically, neither the GNP nor AmberSorb™ 4652 metrics reached the same level of removal at any material loading. While the longer contact-time points do not correspond to practical resident times for in-line configurations, the distribution of the data points is essential to determine scale-up parameters. This chart also informs that GNP still removes TOC faster than the SOA adsorbate; however, it reaches a saturation point faster as well. Nevertheless, the adsorption of TOC by GNP was at least twice as high as the TOC adsorption by AmberSorb™ 4652 at the earlier contact times. Below, the associated linearized isotherm and kinetics diagrams for each adsorbate-contaminant combination are plotted. Note that only the adsorption models that provided the best fit are presented in this section.

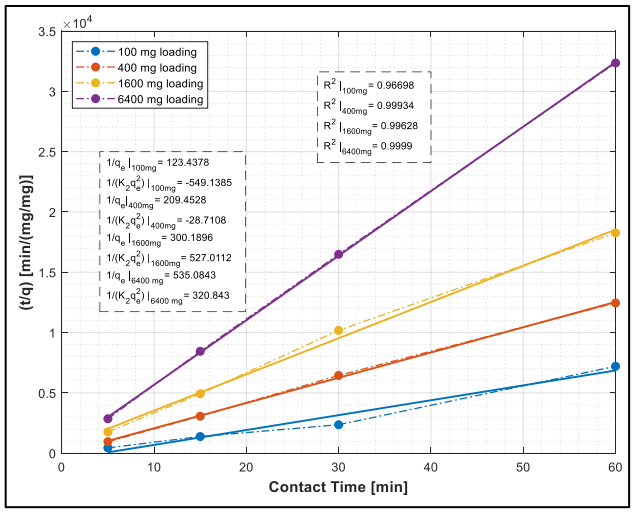

Figure 7. Linearized pSeudo-2nd Order Kinetics - NH4+ Adsorption by GNP.

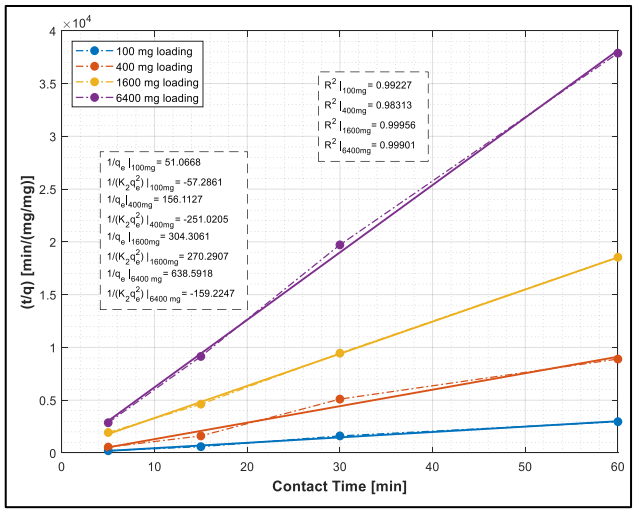

Figure 8. Linearized pSeudo-2nd Order Kinetics - TIC Adsorption by GNP.

Figures 7, 8, 9 showcase the extensive adsorption modelling and the respective plots that fit the data, primarily for GNP. The results for all adsorbents are summarized in Table 2. The adsorption of NH_4^+ and TIC by GNP was predominantly described by *pSeudo-2nd Order* kinetics, with a 0.9999 and 0.9996 coefficient of determination (R^2), respectively. On the other hand, the adsorption process for some contaminants better matched the *Langmuir* model when Granulated Graphene and UltraClean™ UCW 3600 were the adsorbents. However, the corresponding R^2 values were below 0.9. It is worth noting that Kinetics-based modelling offers more reference points since more than one adsorbate loadings can be simultaneously used to compare the regression characteristics. Contrarily, Isotherm-based modelling can only be carried out with the single array of data representing equilibrium points. Moreover, during the regression analysis, the values of the slope and y-axis intercept needed to be carefully assessed. Most of the models in Table 1 predict a positive value for these parameters, with the exception of the *pseudo-1st order* kinetic model. Therefore, regression coefficients were discarded when the values did not match the expected trend even if their respective R^2s were close to a value of one. For example, some data generated a linear correlation, but the corresponding y-axis intercept or the slope did not have physiochemically-possible value (negative magnitudes). These underperforming results are not presented in Tablet 2.

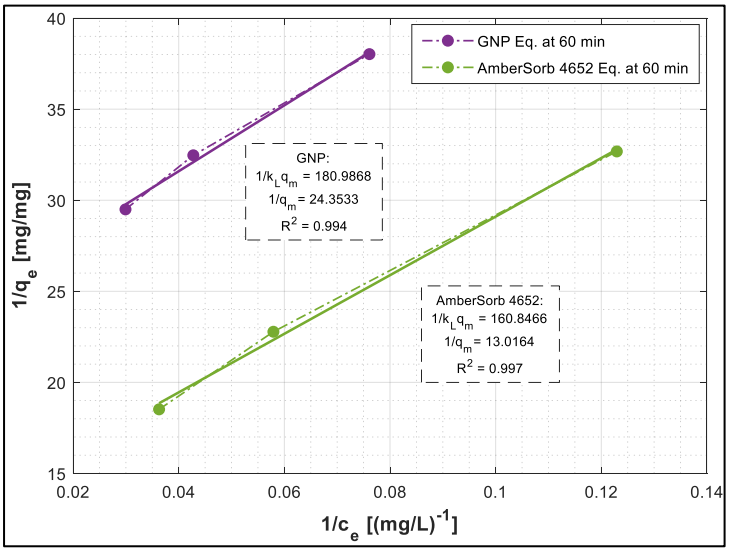

Figure 9. Linearized Langmuir-1 Isotherms - TOC Adsorption by GNP and AmberSorb™ 4652.

Figure 7 shows that the best-fit for NH_4^+ adsorption was provided by the 6400-mg loading experiment while Figure 8 indicates that TIC adsorption was best described by the 1600-mg experiment. These results reveal that GNP has a higher q_e for TIC than for NH_4^+. Nevertheless, the corresponding K_2 values suggest that NH_4^+ adsorption might occur at a faster rate. Furthermore, Table 2 displays that the *Langmuir* model best fitted the data for the removal of inorganics mediated by Granulated Graphene and UltraClean™ UCW 3600. It is also important to point out that TOC removal by Granulated Graphene was not detected. The q_{max} values show that Granulated Graphene has less affinity for NH_4^+ and TIC than GNP. Note that modelling of Granulated Graphene-based data generated the worst regression levels. Whereas Granulated Graphene provided the lowest R^2 values, UltraClean™ UCW 3600 produced better regression and increased q_{max} to a magnitude higher than the q_e by GNP and Granulated Graphene. This result confirms the superiority of the SOA adsorbent for the removal of ionic inorganics. It is to be noted that some linearized isotherms plots were omitted for brevity.

Figure 9 combines the linearized isotherms for GNP and AmberSorb™ 4652 solely for the removal of TOC. The plot also contains the values for the respective slope, y-axis intercepts, and R^2. The equilibrium points from the adsorption experiments at different loadings were selected from the 60-min contact-time point. Although samples at a 120-min contact time were collected, the processed data generated similar results. In other words, equilibrium was well defined by 60 minutes of contact time. Despite the statistical constraints imposed by the limited number of data points, Figure 9 shows an acceptable agreement with the linearized model. As it has been noted, certain GNP loadings removed TOC too quickly and/or the final TOC concentrations were under the limit of detection. Also, the available instrumentation does not confidently provide material-weight measurements below 50 mg. Table 2 substantiates that the TOC-based q_{max} for GNP is virtually half that of the SOA adsorbent. In addition, the results reveal that the energy constant related to the heat of adsorption (K_L) is lower for AmberSorb™ 4652. Even though the modelling demonstrated that the SOA adsorbent still performed better than GNP, recall that GNP were tested in its pristine form without any preconditioning or engineering. This realization is remarkable and can provide the foundation for potential optimization paths for graphene-based filtration media. Nevertheless, these adsorption experiments need to be repeated with multi-component contaminant solutions or standardized solutions based on ISS ersatz wastewater stream.

Another important aspect of these results is the effects of nanoplatelet aggregation on the adsorption process. It is known that GNP easily stack on each other in water-based suspensions, and this mechanism reduces the active surface

area of the material.[32] Consequently, the performance of GNP might have been impacted by the loss of active surface area due to aggregation. Although this mechanism can be reduced by adjusting the acidity of the contaminant solution and reducing the GNP load, the experiments did not attempt any pH adjustment in the associated solutions, and the lowest-possible measurable material loading still created saturated GNP suspensions. Future studies will accommodate the necessary testing adjustments to reduce the impact of aggregation on GACT batch experiments, but it most remains clear that this complication is intrinsic to graphene water-based suspension and does not necessarily impact the incarnation of fixed bed with GBM.

Table 2. Isotherm & Kinetics-based Modelling Summary

Adsorbent	Adsorbate	Best-fit Model	R^2	Parameter	
				q_e [mg/mg]	K_2 [mg/(mg min)]
GNP	NH4+	Psudo-2nd Kinetics	0.9999	1.87×10^{-3}	$8.92\times10^{+2}$
GNP	TIC	Psudo-2nd Kinetics	0.9996	3.29×10^{-3}	$3.43\times10^{+2}$
||	||	||	||	q_{max} [mg/mg]	K_L [L/mg]
Granulated Graphene	NH4+	Langmuir	0.8177	1.22×10^{-3}	4.94×10^{-3}
Granulated Graphene	TIC	Langmuir	0.7002	5.51×10^{-4}	1.39×10^{-2}
UltraClean™ UCW 3600	NH4+	Langmuir	0.9484	2.69×10^{-2}	2.63×10^{-1}
UltraClean™ UCW 3600	TIC	Langmuir	0.9731	1.73×10^{-2}	3.99×10^{-1}
GNP	TOC	Langmuir	0.9940	4.11×10^{-2}	1.35×10^{-1}
AmberSorb™ 4652	TOC	Langmuir	0.9969	7.68×10^{-2}	8.09×10^{-2}

Finally, Figures 10 and 11 depict the outcomes of the microbial challenge test, illustrating the logarithmic decrease in bacterial levels at varying contact times per material load. The data presented in these charts demonstrate that a unit reduction signifies a 90% reduction in the initial bacterial count. Moreover, a logarithmic reduction of 2, 3, 4, and so forth, equates to bacterial inactivation rates of 99%, 99.9%, 99.99%, and beyond, respectively. The findings presented in Figures 10 and 11 indicate a strong correlation between material loading and contact time in the level of bacterial inactivation observed. The results demonstrate that the highest levels of inactivation were achieved with the longest contact time and highest material loading. This outcome aligns with the fundamental understanding that increased material quantity and adequate contact time would lead to a more significant impact on bacterial colonies. Specifically, Figure 10 illustrates that GNP achieved a log reduction of approximately 2 after three hours of interaction and a loading of 6400 mg, while AmberSorb™ 4652 (see Figure 11) only achieved a log reduction of approximately 1 under the same conditions. A range of studies have explored the log reduction required for antimicrobial water filters to be effective. Hayward[33] found that lateral flow sand filters achieved log reductions of 2.9 to 5.4 for antibiotic resistance genes, while Sztuk-Sikorska[34] demonstrated the effectiveness of antibacterial fibrous filters in reducing biofouling. Karim[35] reported a median log 10 reduction of E.coli from 1.8 to 2.7 in mineral pot filters, and Lucier[36] found that ceramic filters with silver and copper nanoparticles achieved an additional 2 log removal for bacteria. These studies collectively suggest that effective antimicrobial

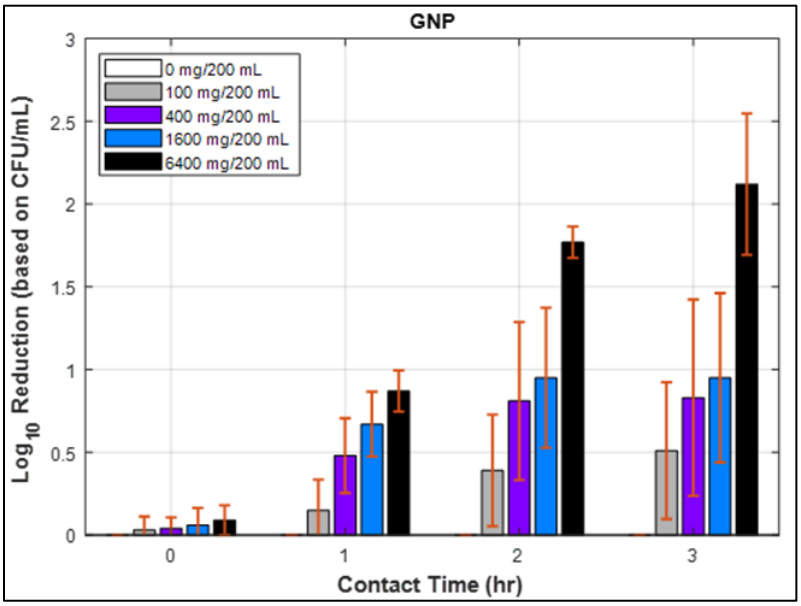

Figure 10. Bacterial Concentration Log Reduction vs. Contact Time – GNP Results.

water filters should aim for log reductions of at least 2 to 5, depending on the specific microorganism being targeted. Notably, the ISS's WPA reduced bacterial concentration up to 4-logs from the wastewater tank to the catalytic oxidizer reactor during its ground qualification test.[37] Although GNP achieved a log reduction close to 2, the corresponding contact time of three hours corresponds to an extreme residence time for LSS water filters. It is imperative to note that the batch-mode microbial challenge utilized in this study was specifically designed for testing antimicrobial properties relying on physiochemical mechanisms, under conditions of moderate mixing. Thus, the results of this initial microbial challenge serve to reaffirm the findings of other studies[38], indicating that water-based GNP suspensions exhibit minimal toxicity towards microorganisms. Flowthrough experiments with GBM-filled pack beds might provide better microbial removal since immobilized nanoplatelets can have a more consistent physical interaction with bacteria, inactivating them via more aggressive physical mechanisms (cell membrane cutting and/or piercing) like some studies suggest.[39,40] Nevertheless, the finding that GNP demonstrates better microbial suppression compared to the SOA material is significant and merits further investigation.

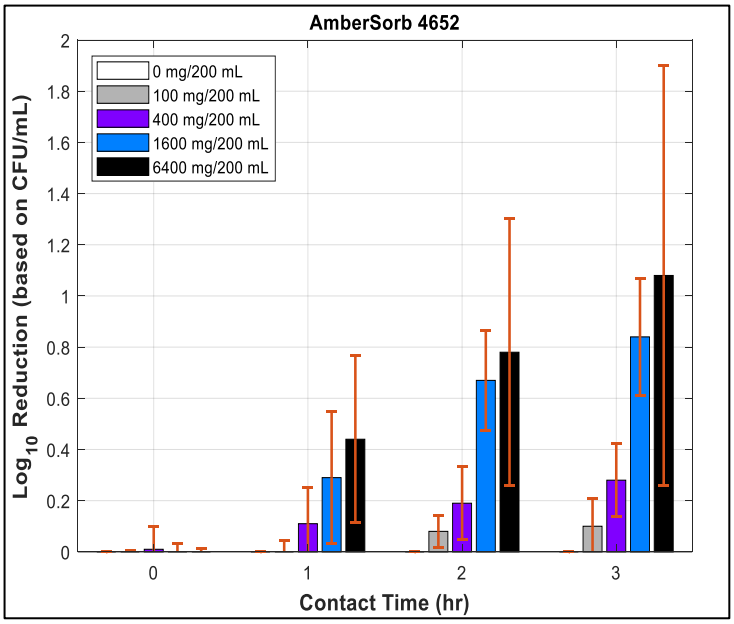

Figure 11. Bacterial Concentration Log Reduction vs. Contact Time – AmberSorb™ 4652 Results.

IV. Conclusions

In conclusion, the research conducted in this study compared the performance of SOA adsorbents with graphene and GBM in removing organic and inorganic contaminants from water. The results indicated that the UltraClean™ UCW 3600 outperformed GNP and Granulated Graphene in removing inorganic contaminants. However, GNP exhibited comparable performance to AmberSorb™ 4652 in removing TOC. This result is highly promising since GNP did not undergo any preconditioning or engineering process prior to testing. Moreover, this investigation provided preliminary testing of the antimicrobial properties of graphene with a relevant bacterial strain found in the ISS's WPA system. While the three-hour contact time required for GNP to achieve a log reduction close to 2 may be impractical for water filters, the study confirmed a measurable level of microbial inhibition and/or removal by GNP towards compared with an SOA spacecraft water filtration material. Further research on flowthrough experiments with GBM-filled pack beds is warranted to explore more aggressive physical mechanisms for microbial removal. This comparison of metrics between these materials has established a relevant performance baseline for graphene and SOA filtration media, and it opens up possibilities for further technological development. By understanding how graphene performs in its pristine state and comparing it with existing adsorbents, this investigation has provided a better understanding of potential paths for optimization, either through preconditions or integration with other particles. The isotherm and kinetics-based modeling has generated a matrix of parameters that can be deployed in geometry-based Multiphysics modeling for the design and simulation of realistic filtration components. The research team plans to further investigate the performance of GBM with multicomponent contaminant solutions (WPA-based ersatz streams) and explore the in-house preparation of graphene-infused filtration media with matrix materials such as resins, foams, composites, hydrogels, etc. SOA filtration media will also be infused with graphene to examine potential enhancement in performance. By immobilizing GNP on other particles, the effects of nanoplatelet aggregation on adsorption can be prevented, and the high-pressure drops associated with fine particles can be avoided while physical antibacterial mechanisms can be enhanced; especially, with flowthrough testing. Through this work, the next generation of ultra-high-capacity filtration media for spacecraft WRS applications are hoped to be realized. Future papers will present

updates on the generation of a series of novel graphene-loaded particle materials applied to testing in flow-through configurations.

V. Acknowledgement

The authors would like to acknowledge and thank the National Aeronautics and Space Administration's Center Innovation Fund for their interest and support of this research. Additionally, the Johnson Space Center Water Technology Development Group would like to express their appreciation to the U.S. Army Engineer Research and Development Center for their valuable collaboration on this project. Moreover, the research group wants to thank Audry Almengor and Hang Nguyen from the Biomedical Research and Environmental Sciences Division's Microbiology Laboratory at the Johnson Space Center for providing support with the microbial challenge test. Finally, the lead author's appreciation goes to Leopoldo Romero & Chris Carrier (JSC EC3 Water Analysis Lab), Ryan Dippolito (NASA Pathways Intern), Stacey Marshall, Phillip Hicks, and Dean Muirhead (JSC EC3 Water Technology De. GRP.) for their extensive contribution to the execution of this investigation.

VI. References

[1]Novoselov, K. S., Geim, A. K., Morozov, S. V., et al. "Electric Field Effect in Atomically Thin Carbon Films," *Science*, V. 306, No. 5696, 2004, pp. 666–9.

[2]Zhang, Y., Tang, T.-T., Girit, C., et al. "Direct observation of a widely tunable bandgap in bilayer graphene," *Nature*, V. 459, No. 7248, 2009, pp. 820–3.

[3]Blake, P., Brimicombe, P. D., Nair, R. R., et al. "Graphene-based liquid crystal device," *Nano letters*, V. 8, No. 6, 2008, pp. 1704–8.

[4]Balandin, A. A., Ghosh, S., Bao, W., et al. "Superior thermal conductivity of single-layer graphene," *Nano letters*, V. 8, No. 3, 2008, pp. 902–7.

[5]Booth, T. J., Blake, P., Nair, R. R., et al. "Macroscopic graphene membranes and their extraordinary stiffness," *Nano letters*, V. 8, No. 8, 2008, pp. 2442–6.

[6]Schedin, F., Geim, A. K., Morozov, S. V., et al. "Detection of individual gas molecules adsorbed on graphene," *Nature materials*, V. 6, No. 9, 2007, pp. 652–5.

[7]Zetterholm, S. G., Gurtowski, L., Roberts, J. L., et al. "Graphene-Mediated removal of Microcystin-LR in chitosan/graphene composites for treatment of harmful algal blooms," *Chemosphere*, V. 300, 2022, p. 134583.

[8]Al-Khateeb, L. A., Almotiry, S., and Salam, M. A. "Adsorption of pharmaceutical pollutants onto graphene nanoplatelets," *Chemical Engineering Journal*, V. 248, 2014, pp. 191–9.

[9]Lazar, P., Karlický, F., Jurecka, P., et al. "Adsorption of small organic molecules on graphene," *Journal of the American Chemical Society*, V. 135, No. 16, 2013, pp. 6372–7.

[10]Kumar, V., Lee, Y. S., Shin, J. W., et al. "Potential applications of graphene-based nanomaterials as adsorbent for removal of volatile organic compounds," *Environment International*, V. 135, 2020, p. 105356.

[11]Sivakumar, M., Widakdo, J., Hung, W. S., et al. "Porous graphene nanoplatelets encompassed with nitrogen and sulfur group for heavy metal ions removal of adsorption and desorption from single or mixed aqueous solution," *Separation and Purification Technology*, V. 288, 2022, p. 120485.

[12]Yang, A., Yang, P., and Huang, C. P. "Preparation of graphene oxide–chitosan composite and adsorption performance for uranium," *Journal of Radioanalytical and Nuclear Chemistry*, V. 313, No. 2, 2017, pp. 371–8.

[13]Brancato, V., Piperopoulos, E., Mastronardo, E., et al. "Synthesis and Characterization of Graphite Composite Foams for Oil Spill Recovery Application," *Journal of Composites Science*, V. 4, No. 4, 2020, p. 154.

[14]Abolhassani, M., Griggs, C. S., Gurtowski, L. A., et al. "Scalable Chitosan-Graphene Oxide Membranes: The Effect of GO Size on Properties and Cross-Flow Filtration Performance," *ACS omega*, V. 2, No. 12, 2017, pp. 8751–9.

[15]Omran, B., and Baek, K. H. "Graphene-derived antibacterial nanocomposites for water disinfection: Current and future perspectives," *Environmental Pollution*, V. 298, 2022, p. 118836.

[16]Ji, H., Sun, H., and Qu, X. "Antibacterial applications of graphene-based nanomaterials: Recent achievements and challenges," *Advanced Drug Delivery Reviews*, V. 105, 2016, pp. 176–89.

[17]Zhou, H., Zou, F., Koh, K., et al. "Antibacterial Activity of Graphene-Based Nanomaterials," *Advances in experimental medicine and biology*, V. 1351, 2022, pp. 233–50.

[18]Molina, M. "Graphene Loop Heat Pipe testing." 46th International Conference on Environmental Systems, 2016.

[19]Kayatin, M. J., Carter, D. L., Schunk, R. G., et al. “Upgrades to the ISS water recovery system.” International Conference on Environmental Systems. 2016.

[20]Williamson, J., Gleich, A., and Wilson, J. “Status of ISS Water Management and Recovery,” 2022.

[21]Kamedulski, P., Skorupska, M., Binkowski, P., et al. “High surface area micro-mesoporous graphene for electrochemical applications,” *Scientific Reports*, V. 11, No. 1, 2021, p. 22054.

[22]Zhang, L., Zhang, F., Yang, X., et al. “Porous 3D graphene-based bulk materials with exceptional high surface area and excellent conductivity for supercapacitors,” *Scientific reports*, V. 3, No. 1, 2013, p. 1408.

[23]Langmuir, I. “The adsorption of gases on plane surfaces of glass, mica and platinum.,” *Journal of the American Chemical society*, V. 40, No. 9, 1918, pp. 1361–403.

[24]Freundlich, H. “Over the adsorption in solution,” *J. Phys. chem*, V. 57, No. 385471, 1906, pp. 1100–7.

[25]Lagergren, S. K. “About the theory of so-called adsorption of soluble substances,” *Sven. Vetenskapsakad. Handingarl*, V. 24, 1898, pp. 1–39.

[26]Yuh-Shan, H. “Citation review of Lagergren kinetic rate equation on adsorption reactions,” *Scientometrics*, V. 59, No. 1, 2004, pp. 171–7.

[27]Ho, Y.-S., and McKay, G. “Pseudo-second order model for sorption processes,” *Process biochemistry*, V. 34, No. 5, 1999, pp. 451–65.

[28]Fierro, V., Torné-Fernández, V., Montané, D., et al. “Adsorption of phenol onto activated carbons having different textural and surface properties,” *Microporous and mesoporous materials*, V. 111, Nos. 1–3, 2008, pp. 276–84.

[29]Weber Jr, W. J., and Morris, J. C. “Kinetics of adsorption on carbon from solution,” *Journal of the sanitary engineering division*, V. 89, No. 2, 1963, pp. 31–59.

[30]Muirhead, D., Moller, S., Adam, N., et al. “A Review of Baseline Assumptions and Ersatz Waste Streams for Partial Gravity Habitats and Orbiting Microgravity Habitats,” 2022.

[31]Westhoff Larner, K., McPhail, C., and Romero, C. “Optimization of a Deionization Bed for an Oxygen Generator Assembly for Exploration Missions,” 2022.

[32]Rosli, F. A., Ahmad, H., Jumbri, K., et al. “Efficient removal of pharmaceuticals from water using graphene nanoplatelets as adsorbent,” *Royal Society Open Science*, V. 8, No. 1, 2021.

[33]Hayward, J. L., Huang, Y., Yost, C. K., et al. “Lateral flow sand filters are effective for removal of antibiotic resistance genes from domestic wastewater,” *Water Research*, V. 162, 2019, pp. 482–91.

[34]Sztuk-Sikorska, E., and Gradoń, L. “Biofouling reduction for improvement of depth water filtration. Filter production and testing,” *Chemical and Process Engineering*, V. 37, 2016, pp. 319–30.

[35]Karim, R., Rahman, S., Hossain, M. A., et al. “Microbiological effectiveness of mineral pot filters as household water treatment in the coastal areas of Bangladesh,” *Microbial Risk Analysis*, V. 4, 2016, pp. 7–15.

[36]Lucier, K. J., Dickson-Anderson, S. E., and Schuster-Wallace, C. J. “Effectiveness of silver and copper infused ceramic drinking water filters in reducing microbiological contaminants,” *Journal of Water Supply Research and Technology-aqua*, V. 66, 2017, pp. 528–36.

[37]Carter, L., Tabb, D., Tatara, J. D., et al. “Performance Qualification Test of the ISS Water Processor Assembly (WPA) Expendables.” SAE International, 2005.

[38]Hu, W., Peng, C., Luo, W., et al. “Graphene-Based Antibacterial Paper,” *ACS Nano*, V. 4, No. 7, 2010, pp. 4317–23.

[39]Akhavan, O., and Ghaderi, E. “Toxicity of Graphene and Graphene Oxide Nanowalls Against Bacteria,” *ACS Nano*, V. 4, No. 10, 2010, pp. 5731–6.

[40]Kang, S., Herzberg, M., Rodrigues, D. F., et al. “Antibacterial Effects of Carbon Nanotubes: Size Does Matter!,” *Langmuir*, V. 24, No. 13, 2008, pp. 6409–13.